RSC Chemical Biology

ROYAL SOCIETY OF CHEMISTRY

PAPER

Published on 26 September 2026
Licensed under CC-BY-NC 4.0

Check for updates

Cite this: *RSC Chem. Biol.*, 2026, 7, 2285

"MIDA masking" of boronic acid therapeutics for enhanced stability and economy

Forrest G. FitzGerald,[a] Jasmin M. Frei,[a] Erika Zhang,[a] Oscar J. Molina,[b] JoLynn B. Giancola,[a] Malo Le Chevalier,[a] Volga Kojasoy[a] and Ronald T. Raines *[ac]

Received 23rd September 2026,
Accepted 24th September 2026

DOI: 10.1039/d6cb00308g

rsc.li/rsc-chembio

Boronic acids are invaluable chemical reagents that enable the synthesis of complex organic molecules and are uniquely leveraged by medicinal chemists to target biological nucleophiles *via* an electrophilic boron center, thereby functioning as reversible covalent inhibitors. Despite their prevalence, boronic acids remain difficult to purify and are notoriously unstable in the presence of air, moisture, and reactive oxygen species—a major impediment to biological applications. We reasoned that the boronic acid protecting group *N*-methyliminodiacetic acid (MIDA), typically restricted to synthetic organic chemistry, could offer a superior protection strategy for boronic acid-containing bioactive molecules. Using the FDA-approved anticancer proteasome inhibitors bortezomib and ixazomib as proof-of-concept substrates, we demonstrate a several-hundred-fold increase in hydrolytic stability of a MIDA boronate compared to the current standard (*e.g.*, diols and α-hydroxy acid protecting groups), imparting significant resistance to oxidation and photodegradation while minimally impacting the biological activity of the molecules in cellular assays. We propose that incorporating MIDA boronates into the synthetic routes of boronic acid-containing drugs could eliminate costly deprotection and reformulation steps in pharmaceutical development, enabling a more direct route to shelf-stable "MIDA-masked" boronic acid medicines.

Introduction

Despite their wide use in organic chemistry,[1–3] materials science,[4–6] and biology,[7–11] boronic acids are sensitive. The Lewis acidity of boron that drives its unique reactivity also makes it susceptible to B–C bond cleavage *via* oxidative deboronation or protodeboronation.[12–16] Chemists have designed protecting groups to withstand harsh chemical reaction conditions, ease purification, and enable long-term storage, yet these strategies perform best in the absence of air and moisture.[17,18] Aqueous conditions and oxidative stress in biological environments remain largely unaddressed, as boronic acid protecting groups designed for organic synthesis are generally too hydrophobic and hydrolytically unstable. In contrast, boronic acid protecting groups designed for biological use (*e.g.*, sugar alcohols or α-hydroxy acids) are incompatible with chemical synthesis and too hydrolytically labile, often requiring excess quantities to counteract reversible diol-boronate exchange.[19,20]

The commercial success of the proteasome inhibitor bortezomib as a frontline therapeutic for multiple myeloma over the past two decades has established boronic acids as valued pharmacophores in targeted covalent drug discovery.[21–23] Yet few boronic acid-containing drugs have achieved similar success. In the clinic, bortezomib is resuspended from a lyophilized formulation containing mannitol and is rapidly administered intravenously or subcutaneously,[24] thereby avoiding first-pass metabolism and targeting an accessible, highly sensitive population of circulating cancer cells. Most of the administered compound is deposited in red blood cells until release and subsequent oxidative metabolism by hepatic CYP3A4 and CYP2C19.[25] The robust glycosylation (*e.g.*, sialylation[26,27]) of red blood cells, coupled with their abundance (*i.e.*, 4-fold greater than all other cells in the body, combined),[28] likely provides a non-specific sink for boronic acid-bearing molecules such as bortezomib to deposit through reversible *cis* 1,2- and 1,3-diol binding interactions. The highly reducing intracellular environment of RBCs, relative to other somatic cells, may protect the pharmacophore from oxidation. Other boronic acid-containing drugs, such as the PDE-4 inhibitor crisaborole, are limited to topical use and formulated with organic solvents to enhance

[a] *Department of Chemistry, Massachusetts Institute of Technology, Cambridge, Massachusetts 02139, USA. E-mail: rtraines@mit.edu*
[b] *Department of Biology, Massachusetts Institute of Technology, Cambridge, Massachusetts 02139, USA*
[c] *Koch Institute for Integrative Cancer Research at MIT, Massachusetts Institute of Technology, Cambridge, Massachusetts 02139, USA*

© 2026 The Author(s). Published by the Royal Society of Chemistry

solubility and limit oxidation.[29,30] A robust and versatile protection strategy is needed to realize the full potential of boronic acid therapeutics, particularly for systemic administration.

An optimal biocompatible boronic acid protecting group should possess the following characteristics: (1) trivalent coordination to boron for enhanced stability, (2) hydrogen-bond donor/acceptor capacity to maintain aqueous solubility, and (3) compatibility with synthetic organic reaction conditions. We identified *N*-methyliminodiacetic acid (MIDA) as a candidate that could accommodate this profile. MIDA has been widely adopted for its stability and selective removal in synthetic organic chemistry applications (*e.g.*, iterative synthesis of small molecules), as well as its hydrolytic stability at neutral-to-acidic pH.[17,31,32]

Nonetheless, few studies have examined the biological utility of MIDA boronates. Llona-Minguez, Helleday, and their coworkers were arguably the first to leverage MIDA derivatization to improve the absorption, distribution, metabolism, and excretion (ADME) properties and plasma stability of a boronic acid inhibitor *in vivo*, observing similar target-binding activity for the protected and unprotected forms.[33] In another study, a small-molecule library used MIDA boronates as reactive handles in an activity-based protein profiling (ABPP) screen against a serine hydrolase.[34] Both studies found similar binding affinities for their protein targets between the MIDA-protected and unprotected boronic acid inhibitors, suggesting that the MIDA group must be hydrolyzed for these molecules to be active inhibitors. A related strategy has been proposed to deliver a boronic acid theranostic *via* MIDA hydrolysis,[35] though the invoked acid-selective release is difficult to reconcile with the well-established base-lability of MIDA boronates.[17,36] To our knowledge, studies evaluating the hydrolytic stability of MIDA boronates in a pharmaceutically relevant context are lacking, as are studies on the impact of MIDA protection on pharmacophore activity or susceptibility to degradation.

In this work, we synthesize and evaluate MIDA-protected analogues of bortezomib (**BTZ**) (Fig. 1) and ixazomib (**IXZ**), two FDA-approved alkylboronic acid-containing proteasome inhibitors. We provide the first detailed analysis of the hydrolytic stability of a MIDA boronate pharmacophore and its ability to protect the boronic acid moiety from oxidation and photodegradation, and we confirm that the cytotoxic activity of the pharmacophore is not hampered *in cellulo*.

Results and discussion

Synthetic strategies

Because alkyl boronic acids such as **BTZ** and **IXZ** are inherently unstable, we used milder conditions[37] than the traditional methods involving high temperatures (*e.g.*, Dean–Stark azeotrope removal[38]) to install the MIDA protecting group. A screen of anhydrous organic solvents identified DMSO as optimal, and DMSO carryover was minimized by using only the volume needed to dissolve the starting materials. We achieved successful MIDA installation on **BTZ** (99% yield) in anhydrous DMSO (Scheme 1). To prepare MIDA-protected **IXZ**, we selected **IXZ**–citrate as the starting material because of its lower cost than unprotected **IXZ**. After citrate deprotection with potassium carbonate, we similarly accessed **IXZ–MIDA** in good yield (85%). As is commonly observed for MIDA boronates, **BTZ–MIDA** and **IXZ–MIDA** were easily purified by silica column chromatography. Although the solid white products were stored under N_2(g) at −20 °C and protected from light—in accordance with the recommendations for unprotected **BTZ** and **IXZ**—no degradation was observed even when the MIDA-protected analogues were stored at room temperature without light shielding.

To properly analyze the oxidation reactions of **BTZ** and **IXZ**, we also needed to isolate and characterize the oxidation products. We adapted a method[39] using H_2O_2 in dimethyl carbonate to selectively generate the oxidation products in high yield for characterization. Interestingly, as observed in our analytical assays, oxidation of **BTZ** generates two diastereomeric products, which we isolated as a mixture by flash chromatography. Preparative TLC was required to separate and isolate the two diastereomers for individual characterization. When generating the oxidation products synthetically, LC-MS showed a diastereomeric ratio of approximately 10 : 1 (**BTZ**-ox-1 : **BTZ**-ox-2), with **BTZ**-ox-1 eluting earlier than **BTZ**-ox-2 during reversed-phase chromatography (Fig. S6 and S7). In our oxidation assays,

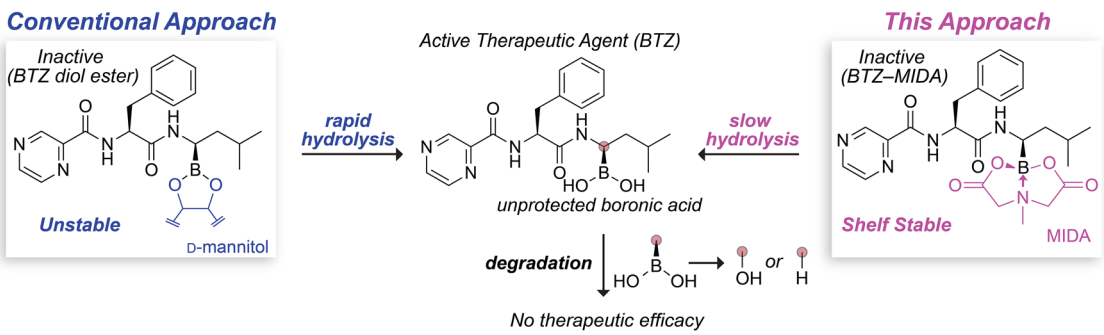
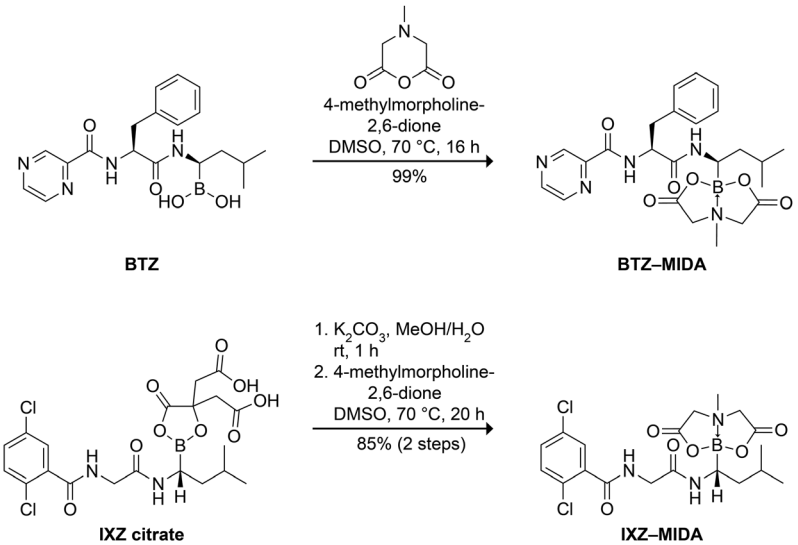


Fig. 1 MIDA masking offers a superior protection strategy for boronic acid therapeutics. Compared to conventional diol-based protecting groups, which are hydrolytically labile and incompatible with synthetic organic chemistry, the MIDA boronate enables slow hydrolytic release, enhanced oxidative stability, and retained pharmacological potency.

© 2026 The Author(s). Published by the Royal Society of Chemistry



Scheme 1 Synthetic routes to MIDA-protected bortezomib (**BTZ–MIDA**) and ixazomib (**IXZ–MIDA**) from commercial starting materials.

however, we did not observe such a drastic ratio, although **BTZ**-ox-1 still predominated. Oxidation of **IXZ** yielded only a single detectable diastereomer, as determined *via* LC-MS (Fig. S12).

Hydrolysis studies

Boronic acid complexation with *cis* 1,2- and 1,3-diols (*e.g.*, glucose, sialic acids, mannitol) and α-hydroxy acids (*e.g.*, citric acid) in aqueous solutions has been extensively studied and used in biosensing applications.[10,40] These interactions are often fast, and without high local concentrations of binding partners, equilibrium favors hydrolysis at neutral pH.[19,20,41] Accordingly, the protecting groups typically used in the synthesis (*e.g.*, pinanediol, pinacol) or reformulation (*e.g.*, mannitol, citric acid) of **BTZ** and **IXZ** are rapidly hydrolyzed upon exposure to aqueous conditions.

We sought to establish the hydrolytic stability of **BTZ–MIDA** across a range of temperatures, pH values, and aqueous media. We developed an LC-MS assay to monitor changes in **BTZ–MIDA** over time, treating boronate ester hydrolysis as a pseudo-first-order reaction. We first compared the hydrolysis of **BTZ**–pinanediol to that of **BTZ–MIDA** in normal saline, a standard solvent for pharmaceutical storage and administration and the solvent of choice for **BTZ** administration. Pinanediol is the most commonly used protecting group in **BTZ** synthesis and represents the penultimate intermediate before deprotection.[42] The half-life ($t_{\frac{1}{2}}$) of **BTZ–MIDA** was 250-fold greater than that of **BTZ**–pinanediol (69 h *versus* ∼0.3 h; Fig. 2A). The addition of mannitol, which is present in the clinical formulation of **BTZ** to aid solubility and prevent boroxine trimer formation,[43] did not alter the half-life, demonstrating that the MIDA ester is resistant to transesterification with diols. In sodium phosphate buffer at pH 7.0, we observed a $t_{\frac{1}{2}}$ of *ca.* 48 h and a trend toward a decreasing half-life with increasing pH, though the effect remained robust. This trend is consistent with the known base-lability of MIDA boronates, which are selectively cleaved under basic conditions in organic synthesis. The MIDA ester was also more stable at a lower temperature (4 °C), and stability can be enhanced *via* chilled storage. Finally, comparing **BTZ–MIDA** with the similarly structured alkyl boronic acid **IXZ–MIDA**, we observed a slight decrease in relative stability ($t_{\frac{1}{2}}$ = 34 h). The phenyl group adjacent to the boron in **BTZ–MIDA** is absent in **IXZ–MIDA**, and we suspect this group provides some steric shielding from hydrolysis in **BTZ–MIDA**.

Oxidation studies

Our primary goal for MIDA protection of boronic acids is to protect the boron moiety from oxidation in biological settings rich in reactive oxygen species (ROS). We chose H_2O_2 as the oxidant because it is the most biologically relevant ROS and, as a two-electron oxidant, it simplifies experimental procedures relative to radical species.[44–46] We devised an LC-MS method to ratiometrically monitor the production of the two diastereomers, **BTZ**-ox-1 and **BTZ**-ox-2, from boronic acid oxidation over time. We first compared oxidation of **BTZ**, **BTZ–MIDA**, and **BTZ**–pinanediol in normal saline (pH 4.0–6.5) and found that after 70 min, 97% of **BTZ** and **BTZ**–pinanediol had been oxidized, whereas only 3% of **BTZ–MIDA** had been oxidized (Fig. S21).

We then evaluated oxidation in phosphate buffer at neutral pH. **BTZ** was completely oxidized within 24 min, whereas only ∼2% of **BTZ–MIDA** oxidized over the same period (Fig. 2B). **IXZ–MIDA** behaved nearly identically to **BTZ–MIDA**, whereas unprotected **IXZ** oxidized faster than **BTZ**, with complete oxidation in the first few minutes. **IXZ** lacks the adjacent phenyl group present in **BTZ**, which may attenuate peroxyanion attack on boron through steric shielding and/or π-donation into the vacant p-orbital (Fig. 3A).

At lower pH, H_2O_2 is more stable, albeit less reactive (*i.e.*, generates a lower concentration of peroxyanion *via* deprotonation), which explains the slower oxidation in normal saline compared to phosphate buffer at pH 7.0. Interestingly, both conditions demonstrate a sigmoidal oxidation profile for **BTZ**–pinanediol. This phenomenon can be explained by an

© 2026 The Author(s). Published by the Royal Society of Chemistry

A *Protecting Group Hydrolysis*

Compound	$t_{1/2}$ (h)	Solvent, Temp.	pH
BTZ–pinanediol	0.258 ± 0.017	saline, rt	4.0–6.5
BTZ–MIDA	68.8 ± 1.1	saline, rt	4.0–6.5
BTZ–MIDA	68.2 ± 0.8	saline + mannitol, rt	4.0–6.5
BTZ–MIDA	10.5 ± 0.2	P_i buffer, rt	8.0
BTZ–MIDA	87.0 ± 1.7	P_i buffer, 4 °C	7.2
BTZ–MIDA	47.6 ± 0.4	P_i buffer, rt	7.0
IXZ–MIDA	34 ± 2	P_i buffer, rt	7.0

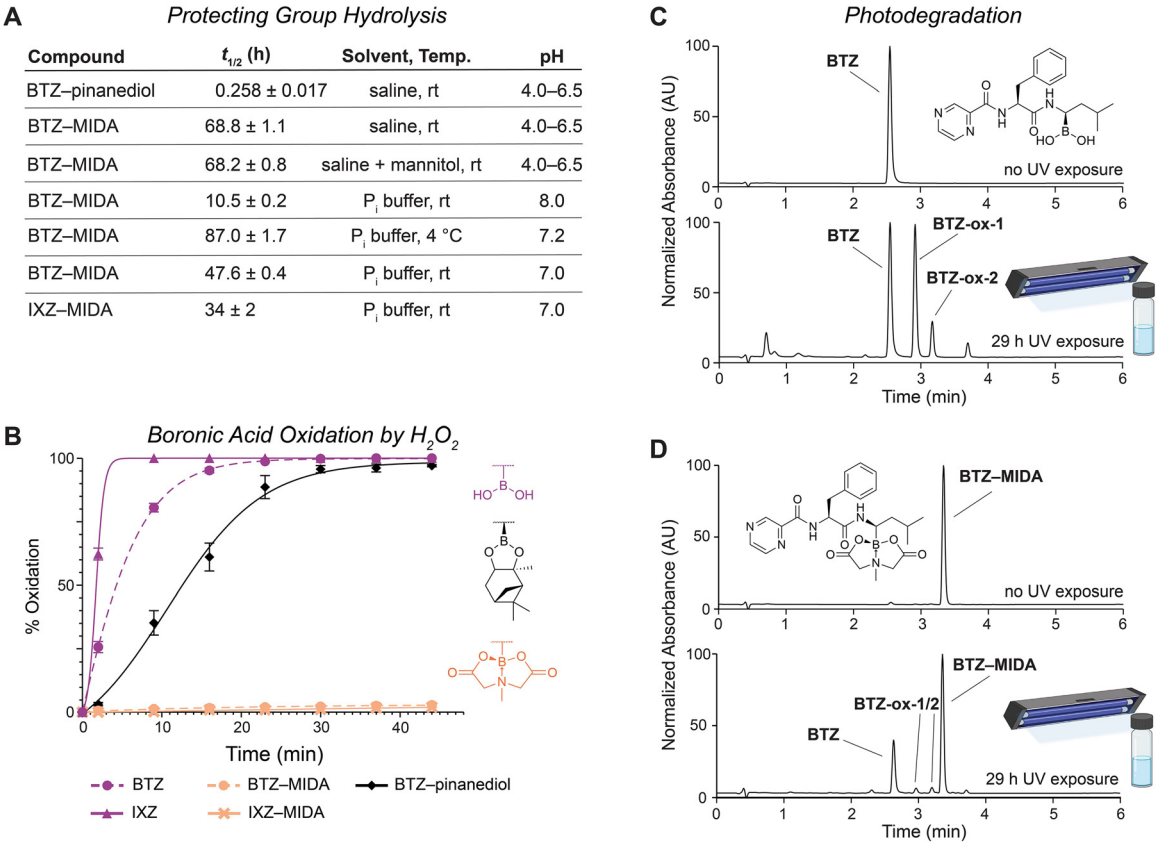


Fig. 2 MIDA protection dramatically enhances the hydrolytic and oxidative stability of **BTZ** and **IXZ**, and the photolytic stability of **BTZ**. (A) Hydrolytic half-lives ($t_{\frac{1}{2}}$, in hours) of **BTZ** and **IXZ** boronate esters under the indicated conditions. (B) Time-dependent oxidation of **BTZ**, **IXZ**, and their protected analogues in the presence of H_2O_2 (330 μM) in 50 mM sodium phosphate buffer, pH 7.0. Values are the mean ± SE for three replicates. (C) Photodegradation of **BTZ** in normal saline under UV irradiation (λ = 254 nm) through borosilicate glass over 29 h. (D) Photodegradation of **BTZ–MIDA** under identical conditions. MIDA protection suppresses the formation of the oxidation products **BTZ**-ox-1 and **BTZ**-ox-2.

initially slow oxidation phase where the pinanediol provides some protection. As **BTZ**–pinanediol rapidly hydrolyzes, oxidation-sensitive **BTZ** is liberated, and the oxidized fraction quickly converges with the profile observed for unprotected **BTZ**.

Photodegradation studies

BTZ undergoes photochemical degradation in solution.[47] We evaluated how UV light (λ = 254 nm) degrades **BTZ** and whether MIDA protection ameliorates this degradation. Using LC-MS, we monitored the degradation of **BTZ** upon exposure to λ = 254 nm and 365 nm using a benchtop UV lamp (Fig. S22). Standard glass vials are made of borosilicate glass, which strongly attenuate short-wavelength (λ = 254 nm) UV light. Because this material is commonly used for compound storage, we first evaluated degradation over the course of 29 h in normal saline using borosilicate vials. The major degradation products, **BTZ**-ox-1 and **BTZ**-ox-2, the two diastereomers from boronic acid oxidation, were apparent (Fig. 2C and Fig. S23).

Repeating the experiment with **BTZ–MIDA** demonstrated minimal production of **BTZ**-ox-1 and **BTZ**-ox-2 after 29 h (Fig. 2D and Fig. S24). The abundance of other degradation products decreased likewise. Using quartz glass containers, which do not filter UV light, we observed greater and more rapid production of degradation products, predominantly with short-wave UV light (Fig. S25–S28). Again, MIDA protection greatly reduced **BTZ** photodegradation. UV-induced photolysis can produce H_2O_2 and hydroxyl radicals in water, although shorter wavelengths ($\lambda \leq 254$ nm) are more efficient.[48] The photolysis is also particularly slow in the absence of a photocatalyst, which informed our experimental design and endpoint selection. These data demonstrate a clear advantage of MIDA protection in preventing light-mediated degradation.

Cytotoxicity studies

BTZ is highly cytotoxic, using an electrophilic boron to form a reversible covalent bond with the side-chain hydroxy group of catalytic threonine in the β5 subunit of the 26S proteasome, causing unfolded proteins to accumulate and aggregate in the cytosol and eventually leading to an apoptotic phenotype.[49,50] Accordingly, **BTZ–MIDA** requires hydrolysis to release the active boronic acid, effectively tuning potency in cells. We observe a ~3-fold increase in IC_{50} for **BTZ–MIDA** relative to **BTZ** in KMS11, a multiple myeloma (MM) cell line. This difference is modest in absolute terms, shifting from 0.42 to 1.22 nM

© 2026 The Author(s). Published by the Royal Society of Chemistry

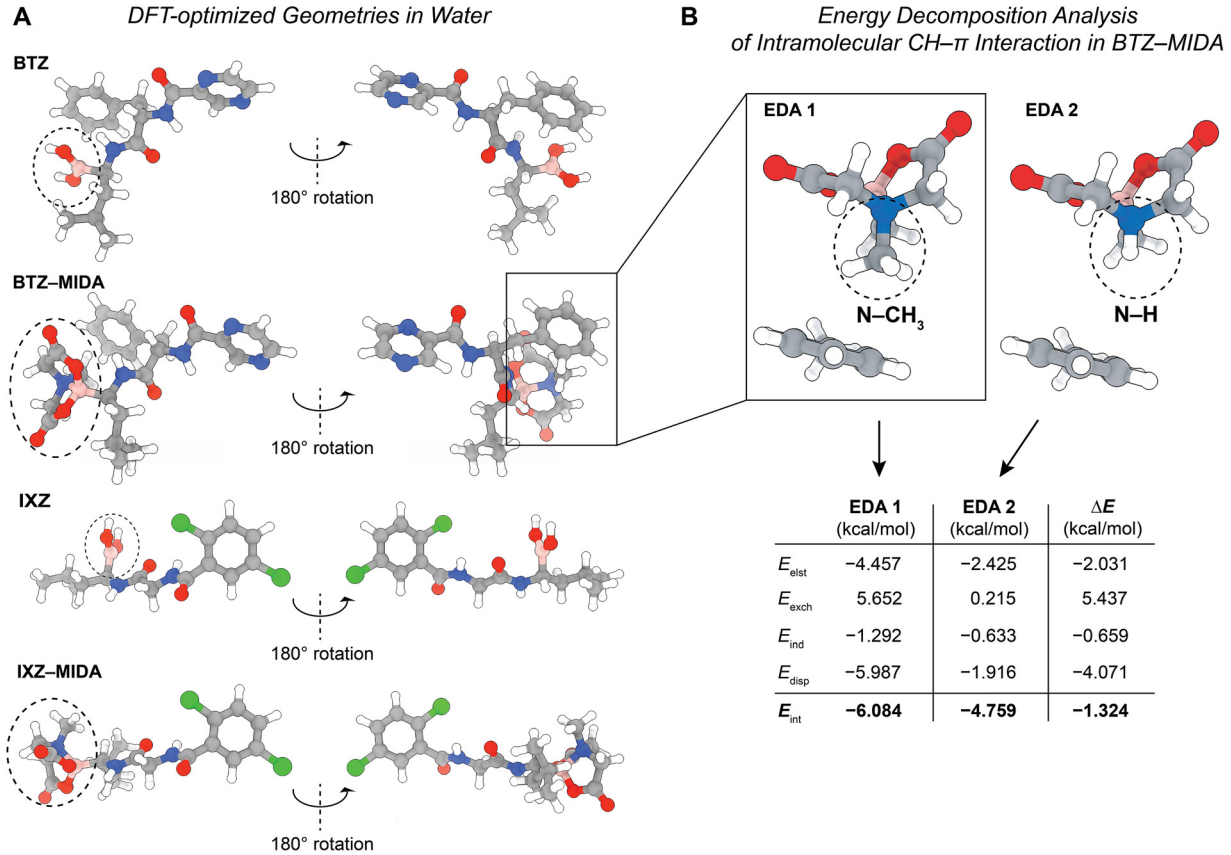


Fig. 3 Computational analysis reveals conformational conservation upon MIDA protection and a stabilizing CH–π interaction in **BTZ–MIDA**. (A) Energy-minimized structures of **BTZ**, **BTZ–MIDA**, **IXZ**, and **IXZ–MIDA** in water, calculated by DFT at the M06-2X/6-31+G(d,p) level with the SMD solvation model.[55–57] Two orientations are shown for each compound; boronic acid and MIDA boronate moieties are circled. Structures were rendered in UCSF ChimeraX.[58] (B) SAPT0 energy decomposition analysis (aug-cc-pVDZ basis set[59,60]) quantifying the intramolecular interaction between the MIDA *N*-methyl group and the **BTZ** phenyl ring. The methylated system (left) is compared to an analogous fragment lacking the *N*-methyl group (right). More negative values indicate stronger stabilizing interactions. Abbreviations: E_{elst}, electrostatic energy; E_{exch}, exchange-repulsion energy; E_{ind}, induction energy; E_{disp}, dispersion energy; E_{int}, total interaction energy.

(Table 1; Fig. S29 and S30). We observed minimal difference for the less potent **IXZ** *versus* **IXZ–MIDA**.

To expand beyond cancer cell lines with well-established sensitivity to proteasome inhibition (*i.e.*, multiple myeloma), we evaluated cytotoxicity in HeLa (cervical cancer) and M21 (melanoma) cell lines. Again, we observed minimal differences in cytotoxicity between the unprotected and MIDA-protected compounds, though these cell lines were less sensitive (Table 1; Fig. S31–S36). MM cells are more sensitive to proteasome inhibition because they contain 10–100-fold fewer proteasomes than most adherent cells[51,52] and overproduce monoclonal immunoglobulins (M proteins), which burden their proteostatic machinery.[53]

Table 1 MIDA protection minimally impacts cytotoxicity in multiple cell lines. IC_{50} values (mean ± SE; n = 3 technical replicates) were determined by an MTS viability assay 48 h after compound treatment

	IC_{50} (nM)		
Compound	KMS11	HeLa	M21
BTZ	0.42 ± 0.04	17.0 ± 1.2	16.9 ± 0.6
BTZ–MIDA	1.22 ± 0.12	25.7 ± 1.4	20.1 ± 1.3
IXZ	1.98 ± 0.30	91.3 ± 8.3	110 ± 5
IXZ–MIDA	2.22 ± 0.45	104 ± 12	85.1 ± 2.2

Because **IXZ**–citrate, rather than free **IXZ**, is the preferred clinical formulation, we compared its cytotoxicity to that of unprotected **IXZ** in HeLa cells. A slight increase in potency was observed (Fig. S33), possibly attributable to improved initial solubility conferred by the citrate moiety, which itself rapidly hydrolyzes in aqueous media. Cytotoxicity is attributable entirely to the unmasked boronic acid, as MIDA alone was not cytotoxic (Fig. S31).

To further confirm the mechanism of action of **BTZ–MIDA**, we directly compared proteasome activity using a chymotrypsin-like fluorescent proteasome substrate in HAP1 cell lysates treated with **BTZ**, **BTZ–MIDA**, or MIDA. HAP1 is a haploid human leukemia cell line commonly used in genetic engineering and drug discovery.[54] Without inhibition, the substrate was rapidly cleaved. Both **BTZ** and **BTZ–MIDA** significantly impeded proteolytic cleavage of the substrate (Fig. S37), though **BTZ** induced greater inhibition than **BTZ–MIDA** in a time-course experiment (Fig. S38). MIDA alone did not inhibit the proteasome, and the

© 2026 The Author(s). Published by the Royal Society of Chemistry

substrate was fully cleaved within minutes, indicating that the unprotected form of **BTZ** in **BTZ–MIDA** is responsible for proteasome inhibition. This result is consistent with the premise that **BTZ–MIDA** is not directly inhibitory and must hydrolyze to yield the active boronic acid. Our cytotoxicity experiments, regardless of cell line, required at least 48 h to observe maximal cell death. MIDA protection could improve stability and cell permeability, offsetting the slower hydrolysis rate. Alternatively, cellular esterases could hydrolyze the MIDA ester over time, releasing the active compound *in cellulo*.

To investigate whether the MIDA ester is susceptible to esterase-mediated hydrolysis, we incubated **BTZ–MIDA** with pig liver esterase (PLE), human paraoxonase/arylesterase 1 (PON1), and human carboxylesterases 1 and 2 (CES1/2)—esterases with broad substrate compatibility. Although hydrolysis increased most with CES2, the effect was marginal and could not be confidently attributed to enzymatic catalysis (Fig. S39–S42). Compared to typical esterase substrates, the MIDA boronate ester is very constrained. Moreover, in typical ester hydrolysis, the leaving group is released before water enters the active site to deacylate the enzyme–substrate intermediate. In the cyclic MIDA boronate, however, the leaving group remains tethered, potentially occluding water access to the active-site nucleophile. More studies are needed to determine whether the MIDA boronate ester is susceptible to esterase-mediated hydrolysis, possibly by other endogenous esterases.

Computational modeling of molecular structures

To determine whether the addition of the MIDA protecting group may impact the preferred conformation of each compound in aqueous conditions, we applied density functional theory (DFT) to calculate energy-minimized structures in water (Fig. 3A). Surprisingly, the overall conformation of **BTZ–MIDA** remained largely unchanged relative to **BTZ**, despite the steric bulk of the MIDA group adjacent to the phenyl ring. In the energy-minimized structure of **BTZ**, the planar face of the trigonal boronic acid stacks against the π-face of the adjacent phenyl ring, positioning the empty p-orbital of boron for potential stabilization by the electron-rich π-face of the adjacent aromatic ring (Fig. 3A and Fig. S43).

Once the MIDA group is added, the core peptide backbone of **BTZ** twists slightly to accommodate the added steric bulk, but not to the extent expected, because the sp^3-hybridized boron no longer seeks stabilization from the adjacent phenyl group. Rather, the *N*-methyl group of MIDA faces the π-face of the phenyl ring, suggesting that a CH–π interaction stabilizes this energy-minimized conformation in water (Fig. 3 and Fig. S44).

To quantify the potential contribution of the CH–π interaction, we performed an energy decomposition analysis using symmetry-adapted perturbation theory (SAPT)[61–64] and compared the interaction energies between the phenyl and MIDA groups with and without the *N*-methyl moiety. Although the methyl group introduces appreciable steric repulsion, as reflected in the large exchange energy (E_{exch}), the attractive electrostatic (E_{elst}) and dispersion (E_{disp}) contributions outweigh it, yielding a net

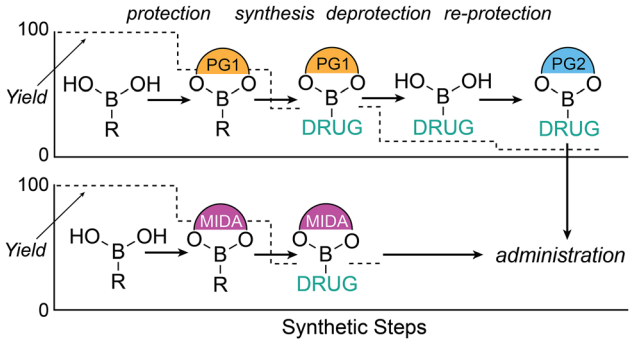


Fig. 4 MIDA compatibility with both synthetic chemistry and biological systems reduces the number of steps required to produce shelf-stable boronic acid therapeutics. In a conventional route (top), a synthesis-compatible protecting group (PG) must be removed and replaced with a biology-compatible PG prior to formulation. With MIDA masking (bottom), MIDA serves as a single protecting group throughout synthesis, purification, and formulation, eliminating the need for deprotection and reformulation steps.

stabilization of −1.32 kcal mol^{-1} relative to the unmethylated system (Fig. 3B) at a distance of 3.4 Å between the *N*-methyl carbon and the center of the phenyl ring (Fig. S44). This agrees with the fact that CH–π interactions are driven predominantly by dispersion forces.[65]

MIDA has a greater impact on the conformation of **IXZ**. **IXZ** has a linear conformation in water with the trigonal boronic acid positioned perpendicular to the peptide backbone and is solvent-exposed (Fig. 3A). Upon the addition of MIDA, there is a major twist at the C_α attached to the boron, positioning the adjacent isopropyl group perpendicular to the linear conformation of the peptide backbone. In the absence of predictable stabilizing interactions, as observed in **BTZ** and **BTZ–MIDA**, **IXZ–MIDA** remains highly flexible. These findings provide insight into the structural impact of MIDA masking on small-molecule conformation and, ultimately, on stability and permeability. Importantly, in both cases, the MIDA group carbonyls adopt the most solvent-exposed conformation, contributing to aqueous solubility.

Conclusions

MIDA boronates have proven themselves indispensable in synthetic organic chemistry. Here, we provide evidence for a new application of the MIDA protecting group: masking of boronic acid therapeutics for use in biological settings. Using two widely recognized boronic acid-containing drugs, bortezomib and ixazomib, we show that a MIDA-protected analogue is hydrolytically stable and resistant to oxidation and photodegradation. This masking strategy does not significantly alter compound activity *in cellulo* and could additionally prevent non-specific interactions with endogenous diols, including cell-surface carbohydrates. These results may differ depending on the type of therapeutic agent being masked and its target and/or mechanism of action. Therefore, stability and activity

© 2026 The Author(s). Published by the Royal Society of Chemistry

studies, such as those reported herein, should be conducted for each boronic acid therapeutic that uses this MIDA masking approach. Finally, because MIDA boronates are compatible with standard organic synthesis conditions, their use as building blocks should enable facile purification and obviate the deprotection and reformulation steps currently required—steps that reduce yields because unprotected boronic acids are difficult to purify by normal-phase chromatography and are susceptible to protodeboronation and oxidative deboronation. MIDA-masked boronic acid therapeutics could eliminate synthetic steps, thereby improving preparation economy (Fig. 4).

Author contributions

F. G. F.: conceptualization, methodology, investigation, software, formal analysis, validation, writing – original draft, visualization. J. M. F.: methodology, investigation, formal analysis, writing – review and editing. E. Z.: investigation, software, writing – review and editing. O. J. M.: investigation, writing – review and editing. J. B. G.: investigation, writing – review and editing. M. L. C.: investigation, writing – review and editing. V. K.: software, writing – review and editing. R. T. R.: supervision, funding acquisition, writing – review and editing.

Conflicts of interest

There are no conflicts to declare.

Data availability

The data supporting the findings of this study are available within the article and its Supplementary information (SI). The SI includes full experimental procedures, compound characterization data (NMR, HRMS, LC-MS), kinetic analyses of hydrolysis and oxidation, cytotoxicity dose response curves, proteasome activity assays, esterase incubation data, and computational details including optimized geometries and SAPT energy decomposition analyses. See DOI: https://doi.org/10.1039/d6cb00308g.

Acknowledgements

F. G. F. and E. Z. were supported by Graduate Research Fellowships from the National Science Foundation. J. M. F. was supported by the Excellence Scholarship and Opportunity Program (ETH–Zürich). M. L. C. was supported by École normale supérieure Paris–Saclay. This work was supported by Grant R35 GM148220 (NIH) and used computational resources through allocation BIO230178 from the Advanced Cyberinfrastructure Coordination Ecosystem: Services & Support (ACCESS) program, which was supported by Grant ACI 1548562 (NSF). UV lamp and vial illustrations were made with BioRender.com.

Notes and references

1 D. G. Hall, in *Boronic Acids*, ed. D. G. Hall, Wiley-VCH, Weinheim, Germany, 1st edn, 2005, pp. 1–99.
2 J. Li, A. S. Grillo and M. D. Burke, *Acc. Chem. Res.*, 2015, **48**, 2297–2307.
3 B. J. Graham and R. T. Raines, *J. Org. Chem.*, 2024, **89**, 2069–2089.
4 S. K. Mellerup and S. Wang, *Chem. Soc. Rev.*, 2019, **48**, 3537–3549.
5 Y.-Y. Aung, A. N. Kristanti, H. V. Lee and M. Z. Fahmi, *ACS Omega*, 2021, **6**, 17750–17765.
6 F. Zhao, M. An, N. Wang and X. Yin, *Chem. – Eur. J.*, 2025, **31**, e202403810.
7 N. Ni and B. Wang, in *Boronic Acids*, ed. D. G. Hall, Wiley–VCH, Weinheim, Germany, 2nd edn, 2011, pp. 591–620.
8 K. A. Andersen, T. P. Smith, J. E. Lomax and R. T. Raines, *ACS Chem. Biol.*, 2016, **11**, 319–323.
9 B. Akgun and D. G. Hall, *Angew. Chem., Int. Ed.*, 2018, **57**, 13028–13044.
10 G. Fang, H. Wang, Z. Bian, J. Sun, A. Liu, H. Fang, B. Liu, Q. Yao and Z. Wu, *RSC Adv.*, 2018, **8**, 29400–29427.
11 S. A. G. Monteiro, P. M. P. Gois and J. P. M. António, *Synlett*, 2023, 2129–2158.
12 J. Labutti, I. Parsons, R. Huang, G. Miwa, L.-S. Gan and J. S. Daniels, *Chem. Res. Toxicol.*, 2006, **19**, 539–546.
13 J. A. Plumley and J. D. Evanseck, *J. Phys. Chem. A*, 2009, **113**, 5985–5992.
14 A. Bolognese, A. Esposito, M. Manfra, L. Catalano, F. Petruzziello, M. C. Martorelli, R. Pagliuca, V. Mazzarelli, M. Ottiero, M. Scalfaro and B. Rotoli, *Adv. Hematol.*, 2009, **2009**, 704928.
15 E. A. Garcia, D. Pessoa and M. Herrera-Alonso, *Soft Matter*, 2020, **16**, 2473–2479.
16 A. Sikora, J. Zielonka, K. Dębowska, R. Michalski, R. Smulik-Izydorczyk, J. Pięta, R. Podsiadły, A. Artelska, K. Pierzchała and B. Kalyanaraman, *Front. Chem.*, 2020, **8**, 580899.
17 D. M. Knapp, E. P. Gillis and M. D. Burke, *J. Am. Chem. Soc.*, 2009, **131**, 6961–6963.
18 Q. I. Churches and C. A. Hutton, in *Boron Reagents in Synthesis*, ed. A. Coca, American Chemical Society, Washington, DC, 2016, pp. 357–377.
19 N. Ni, S. Laughlin, Y. Wang, Y. Feng, Y. Zheng and B. Wang, *Bioorg. Med. Chem.*, 2012, **20**, 2957–2961.
20 W. L. A. Brooks, C. C. Deng and B. S. Sumerlin, *ACS Omega*, 2018, **3**, 17863–17870.
21 P. F. Bross, R. Kane, A. T. Farrell, S. Abraham, K. Benson, M. E. Brower, S. Bradley, J. V. Gobburu, A. Goheer, S. L. Lee, J. Leighton, C. Y. Liang, R. T. Lostritto, W. D. McGuinn, D. E. Morse, A. Rahman, L. A. Rosario, S. L. Verbois, G. Williams, Y. C. Wang and R. Pazdur, *Clin. Cancer Res.*, 2004, **10**, 3954–3964.
22 P. Robak and T. Robak, *Drugs R&D*, 2019, **19**, 73–92.
23 Faridoon, R. Ng, G. Zhang and J. J. Li, *Med. Chem. Res.*, 2023, **32**, 1039–1062.

© 2026 The Author(s). Published by the Royal Society of Chemistry

24 Velcade [package insert], Millennium Pharmaceuticals, Cambridge, MA, 2003.
25 A. Hemeryck, R. Geerts, J. Monbaliu, S. Hassler, T. Verhaeghe, L. Diels, W. Verluyten, L. van Beijsterveldt, R. N. Mamidi, C. Janssen and R. De Coster, *Cancer Chemother. Pharmacol.*, 2007, **60**, 777–787.
26 I. Kahane, A. Polliack, E. A. Rachmilewitz, E. A. Bayer and E. Skutelsky, *Nature*, 1978, **271**, 674–675.
27 D. Aminoff, J. Anderson, L. Dabich and W. D. Gathmann, *Am. J. Hematol.*, 1980, **9**, 381–389.
28 I. A. Hatton, E. D. Galbraith, N. S. C. Merleau, T. P. Miettinen, B. M. Smith and J. A. Shander, *Proc. Natl. Acad. Sci. USA*, 2023, **120**, e2303077120.
29 G. F. S. Fernandes, W. A. Denny and J. L. Dos Santos, *Eur. J. Med. Chem.*, 2019, **179**, 791–804.
30 P. K. Sahu, J. Panda, V. V. J. K. Yantapalli and L. L. M. Piratla, *SN Appl. Sci.*, 2020, **2**, 598.
31 T. Mancilla, R. Contreras and B. Wrackmeyer, *J. Organomet. Chem.*, 1986, **307**, 1–6.
32 D. J. Blair, S. Chitti, M. Trobe, D. M. Kostyra, H. M. S. Haley, R. L. Hansen, S. G. Ballmer, T. J. Woods, W. Wang, V. Mubayi, M. J. Schmidt, R. W. Pipal, G. F. Morehouse, A. M. E. Palazzolo Ray, D. L. Gray, A. L. Gill and M. D. Burke, *Nature*, 2022, **604**, 92–97.
33 S. Llona-Minguez, A. Höglund, S. A. Jacques, L. Johansson, J. M. Calderón-Montaño, M. Claesson, O. Loseva, N. C. K. Valerie, T. Lundbäck, J. Piedrafita, G. Maga, E. Crespan, L. Meijer, E. Burgos Morón, P. Baranczewski, A.-L. Hagbjörk, R. Svensson, E. Wiita, I. Almlöf, T. Visnes, F. Jeppsson, K. Sigmundsson, A. J. Jensen, P. Artursson, A.-S. Jemth, P. Stenmark, U. Warpman Berglund, M. Scobie and T. Helleday, *J. Med. Chem.*, 2016, **59**, 1140–1148.
34 J. Tan, A. B. Cognetta III, D. B. Diaz, K. M. Lum, S. Adachi, S. Kundu, B. F. Cravatt and A. K. Yudin, *Nat. Commun.*, 2017, **8**, 1760.
35 J. Liu, J. Wang, S. Si, J. Xu and P. Xue, *ChemMedChem*, 2021, **16**, 3231–3235.
36 E. P. Gillis and M. D. Burke, *J. Am. Chem. Soc.*, 2008, **130**, 14084–14085.
37 A. M. Kelly, P.-J. Chen, J. Klubnick, D. J. Blair and M. D. Burke, *Org. Lett.*, 2020, **22**, 9408–9414.
38 B. E. Uno, E. P. Gillis and M. D. Burke, *Tetrahedron*, 2009, **65**, 3130–3138.
39 R. B. Wagh and J. M. Nagarkar, *Tetrahedron Lett.*, 2017, **58**, 4572–4575.
40 G. T. Williams, J. L. Kedge and J. S. Fossey, *ACS Sens.*, 2021, **6**, 1508–1528.
41 G. Springsteen and B. Wang, *Tetrahedron*, 2002, **58**, 5291–5300.
42 A. Rentsch, D. Landsberg, T. Brodmann, L. Bülow, A.-K. Girbig and M. Kalesse, *Angew. Chem., Int. Ed.*, 2013, **52**, 5450–5488.
43 A. Lopalco, R. M. Iacobazzi, N. Denora and V. J. Stella, *J. Pharm. Sci.*, 2021, **110**, 543–547.
44 D. R. Gough and T. G. Cotter, *Cell Death Dis.*, 2011, **2**, e213.
45 C. C. Winterbourn, *Methods Enzymol.*, 2013, **528**, 3–25.
46 A. J. P. O. de Almeida, J. C. P. L. de Oliveira, L. V. da Silva Pontes, J. F. de Souza Júnior, T. A. F. Gonçalves, S. H. Dantas, M. S. de Almeida Feitosa, A. O. Silva and I. A. de Medeiros, *Oxid. Med. Cell. Longevity*, 2022, **2022**, 1225578.
47 P. André, S. Cisternino, F. Chiadmi, A. Toledano, J. Schlatter, O. Fain and J.-E. Fontan, *Ann. Pharmacother.*, 2005, **39**, 1462–1466.
48 K. Guo, S. Wu, W. Qin, R. Xie, Y. Wu, X. Li, G. Ouyang and J. Fang, *Environ. Sci. Technol.*, 2024, **58**, 22431–22441.
49 J. A. M. Bard, E. A. Goodall, E. R. Greene, E. Jonsson, K. C. Dong and A. Martin, *Annu. Rev. Biochem.*, 2018, **87**, 697–724.
50 T. A. Thibaudeau and D. M. Smith, *Pharmacol. Rev.*, 2019, **71**, 170–197.
51 A. Kumatori, K. Tanaka, N. Inamura, S. Sone, T. Ogura, T. Matsumoto, T. Tachikawa, S. Shin and A. Ichihara, *Proc. Natl. Acad. Sci. USA*, 1990, **87**, 7071–7075.
52 K. B. Hendil, R. Hartmann-Petersen and K. Tanaka, *J. Mol. Biol.*, 2002, **315**, 627–636.
53 M. Pelon, P. Krzeminski, Z. Tracz-Gaszewska and I. Misiewicz-Krzeminska, *Front. Pharmacol.*, 2024, **15**, 1351565.
54 G. Llargués-Sistac, L. Bonjoch and S. Castellvi-Bel, *Front. Cell Dev. Biol.*, 2023, **11**, 1111488.
55 Y. Zhao and D. G. Truhlar, *Acc. Chem. Res.*, 2008, **41**, 157–167.
56 Y. Zhao and D. G. Truhlar, *Theor. Chem. Acc.*, 2008, **120**, 215–241.
57 A. V. Marenich, C. J. Cramer and D. G. Truhlar, *J. Phys. Chem. B*, 2009, **113**, 6378–6396.
58 E. C. Meng, T. D. Goddard, E. F. Pettersen, G. S. Couch, Z. J. Pearson, J. H. Morris and T. E. Ferrin, *Protein Sci.*, 2023, **32**, e4792.
59 R. A. Kendall, T. H. Dunning, Jr. and R. J. Harrison, *J. Chem. Phys.*, 1992, **96**, 6796–6806.
60 R. C. Dey, P. Seal and S. Chakrabarti, *J. Phys. Chem. A*, 2009, **113**, 10113–10118.
61 E. G. Hohenstein and C. D. Sherrill, *J. Chem. Phys.*, 2010, **132**, 184111.
62 E. G. Hohenstein, R. M. Parrish, C. D. Sherrill, J. M. Turney and H. F. Schaefer, III, *J. Chem. Phys.*, 2011, **135**, 174107.
63 T. M. Parker, L. A. Burns, R. M. Parrish, A. G. Ryno and C. D. Sherrill, *J. Chem. Phys.*, 2014, **140**, 094106.
64 A. M. Keys, D. W. Kastner, L. L. Kiessling and H. J. Kulik, *Chem. Sci.*, 2025, **16**, 1746–1761.
65 M. Nishio, *Phys. Chem. Chem. Phys.*, 2011, **13**, 13873–13900.

© 2026 The Author(s). Published by the Royal Society of Chemistry